

# Analysis of solar, interplanetary, and geomagnetic parameters during solar cycles 22, 23, and 24

Binod Adhikari<sup>1,2</sup>, Dahal Subodh<sup>3,4</sup>, Roshan Kumar Mishra<sup>1</sup>, Nirakar Sapkota<sup>1</sup>, Daya Nidhi Chhatkuli<sup>5</sup>, Santosh Ballav Sapkota<sup>1</sup>, Sarala Adhikari<sup>5</sup>, and Narayan P. Chapagain<sup>6</sup>

Received 25 April 2018; accepted 20 November 2018; published 31 January 2019.

We have analyzed the trend of solar, interplanetary, and geomagnetic (SIG) parameters during solar cycles 22, 23, and 24. The sunspot numbers ( $R$ ), solar flux index ( $F_{10.7}$ ) and Lyman Alpha ( $L$ ) indicate periodic trend during each solar cycle. In solar cycle 24 sunspot numbers ( $R$ ),  $F_{10.7}$ , and  $L$  show periodic nature, but their peak is low. However, polar cap index (PCI) has maximum value in the latest solar cycle. We found a positive correlation between PCI and polar cap voltage (PCV). This means, during this period, there is a big difference between the maximum and minimum electronic convection potential in the ionosphere. In the solar cycle 24, Sun polar fields had low magnitude compared to cycle 22 and 23. This low solar polar field corresponds to the highest difference between electronic convection potentials. The same low solar polar field also corresponds to low values in  $R$ ,  $F_{10.7}$ , and  $L$ . Through continuous wavelet transform (CWT), we found that solar flux, sunspot number, Lyman Alpha all have highest spectral variability from 0 to 100 months. Sunspot number, Lyman Alpha,  $F_{10.7}$  all have a continuous spectral energy of medium and low magnitude. We suggest that these unique condition of SIG parameters have originated from solar activity.

**KEYWORDS:** Sunspot; solar flux; cross-correlation; wavelet analysis.

**Citation:** Adhikari, Binod, Dahal Subodh, Roshan Kumar Mishra, Nirakar Sapkota, Daya Nidhi Chhatkuli, Santosh Ballav Sapkota, Sarala Adhikari, and Narayan P. Chapagain (2019), Analysis of solar, interplanetary, and geomagnetic parameters during solar cycles 22, 23, and 24, *Russ. J. Earth. Sci.*, 19, ES1003, doi:10.2205/2018ES000645.

## Introduction

Sunspots are dark magnetic areas created in the interior of the Sun. They are continuously observed on the solar surface since 1600s. The solar activity displays periodic variation from days to thousands of years [Kilcik *et al.*, 2014]. The solar cycle is the amount of time from one solar minimum to the next. The detailed study of all solar cycle is necessary to understand the nature of sunspot numbers. The origin of sunspot cycle has been researched for a long time [Chattopadhyay and Chattopadhyay, 2012]. The study of sunspot number and solar activity have been done for more than a century and numerous papers, books and reviews have already

<sup>1</sup>Department of Physics, St. Xavier's College, Maitighar, Kathmandu, Nepal

<sup>2</sup>Department of Physics, Tribhuvan University, Patan Multiple Campus, Lalitpur, Nepal

<sup>3</sup>Department of Physics, Himalayan College of Geomatic Engineering and LRM, Kathmandu, Nepal

<sup>4</sup>Central Department of Physics, Tribhuvan University, Kirtipur, Nepal

<sup>5</sup>Department of Physics, Tribhuvan University, Tri-Chandra Multiple Campus, Kathmandu, Nepal

<sup>6</sup>Department of Physics, Tribhuvan University, Amrit Science Campus, Kathmandu, Nepal

been published [e.g. *Eddy, 2009; Hathaway, 2015*]. Some interesting results related to the long-term variation of sunspot activity have appeared in the last few years [*Usoskin and Mursula, 2003*]. The study of solar activity through sunspot number and their relationship is still a challenge in solar physics. The solar activity and radiation output are associated to space weather, biosphere, technology, and lives on the Earth [*Chattopadhyay and Chattopadhyay, 2012*]. So, these are current theoretical problems having significant practical issues. Predictions have been made about climate change that may result from rise in carbon dioxide and methane levels [*Solomon et al., 2007*]. Even though solar forcing on Earth's climate is an idea that dates back to the XIX century [*Herschel, 1901; Gray et al., 2010*], we have poorly understood how solar variability acts as a forcing mechanism [*Engels and Geel, 2012*]. Periods of low solar variability and their impact on climate have been documented in recent history [*Eddy, 1976*], and the documentation of changes in temperature or precipitation also has a relatively short history. The patterns, as well as timing of past climate change, are necessary to understand what caused the climate change at different timescales [*Vandenberghe et al., 1998*].

Solar radiation entering the atmosphere depends on Earth's position with respect to the Sun and solar activity. *Milankovitch* [1941] was the first to describe the effect of poly-cyclic nature of Earth's position with respect to the Sun on Earth's climate. Such effects are known as orbital forcing. When variation takes place in Earth's eccentricity, obliquity, and precession, major climate change takes place [*Berger, 1988*]. In the last 2.6 Myrs, the effect of eccentricity, precession, and obliquity have caused a dynamic climate characterized by differences between short interglacial periods and relatively long glacial periods [*Engels and Geel, 2012*]. Cyclic changes in the magnetic activity of the Sun results in total solar irradiance (TSI) variations. TSIs on long-scales are superimposed on the orbital-forcing-induced changes. Observations of instrumental data from the last 30 years demonstrate cyclic variations of signals in TSI having a periodicity of about 11 years. The sunspot maximum and minimum have a measured difference in TSI of about  $1 \text{ Wm}^2$  [*Fröhlich, 2006*]. This radiative forcing is small when compared to that caused by greenhouse gases (about  $2.45 \text{ Wm}^2$ ) [*Lockwood,*

*2012*]. Sunspots by themselves never emit radiation of particles that interact with the Earth, but sunspots are markers of the center of activity, hence the variation of sunspot number reveals the activity level of the Sun. This knowledge of past solar activity is vital to Earth [*Jager, 2005*]. This solar activity is considered as the best indicator of the intensity of radiations from the Sun at frequencies in the range of x-rays and ultraviolet. Moreover, the study of solar activity would be interesting for geophysicists, climatologists, and astronomers or solar physicists as they help in better understanding of the Sun.

Generally, solar activity is characterized by any type of natural phenomena that occur on or in the Sun, for instance: solar wind, sunspots, solar flares, coronal mass ejections, etc. Therefore, in order to study the statistical properties of solar activity, we need some numerical characteristics related to the entire Sun that reflect its main feature. Such characteristics are called indices of solar activity [*Usoskin and Mursula, 2003*]. Solar activity variations modulate space phenomena such as highly energetic charged particles, called cosmic rays, coming from the heliosphere. Cosmic rays are affected by the interplanetary magnetic field (IMF) and show a near anti-correlation with sunspot numbers on timescales of the solar cycle period, i.e., 11 years [*Caprioli et al., 2010*]. Many different solar indices or parameters were discovered based on faculae, flares, coronal holes, and electromagnetic radiation in various bands such as 10.7 cm radio flux, sunspots, the total solar irradiance, coronal mass ejections, geo-magnetic activity, galactic cosmic ray fluxes and ice cores.

## Datasets and Methodology

The sunspot numbers, solar flux index, Lyman Alpha, the solar wind datasets and geomagnetic indices used in this work were downloaded from: <https://omniweb.gsfc.nasa.gov/>. Cross-correlation and wavelet analysis have been implemented. Cross-correlation is a measure of statistical relationships between two or more variables as a function of time lags. One can simply understand the cross-correlation as a measure of similarities between two different time series functions, one relative

to the other. The fundamental idea is that a wavelet analyzing function is a localized wave, i.e., it has a fast decay of the amplitude with respect to time or frequency domain [Daubechies, 1992; Grossmann and Morlet, 1983]. We use here the well known Morlet analyzing function that balances time and scale domain representations [Daubechies, 1992; Domingues et al., 2005; Grossmann and Morlet, 1983; Morlet, 1983]. A continuous wavelet transform (CWT) provides redundant and continuous detailed description of a signal in terms of both time and scale.

## Result and Discussion

In this section, we discuss the interplanetary parameter variation in response to sunspot number and their association with phases of three different solar cycle events. The top panel of Figure 1 represents the sunspot number variation during the solar cycle 22, 23 and 24. The solar cycle 22 started in 1986 and had its peak in 1990, decline phase of this period extended from 1992 until 1995. During the rising phase (1986–1988) of this cycle, the sunspot number increases from minimum value around 45 to almost constant during maximum phase (1988–1992), acquiring the maximum value of sunspots, i.e., 240 in the year 1990. During its declining phase (1992–1995) this value falls to 40 in 1995.

The solar cycle 23 started in 1996 and had its peak in early 2000–01 and decline phase of this period extended from 2002 to 2009. Solar cycle 23 rises slowly in the beginning, depicting a smooth maxima between 1999 and 2002 acquiring the maximum value of sunspots, i.e., 200 in the year 2000 which is the largest in the 23rd cycle and then declines to 54 in 2006. The sunspot numbers observed during the start and end phases of the solar cycle are almost same (i.e. 57 and 54 in 1996 and 2006 respectively). Solar cycle 23 had a rising phase from 1996 to 1998, a maximum phase from 1999 to 2002 and a declining phase from 2003 to 2006. Thus, it is implied that solar cycle 23 started from the minimum activity of sunspot numbers in 1996, attaining maximum value in 2000 and falling back to almost the same activity of sunspot numbers in 2006. The solar cycle 24 started in 2009 and had its peak in 2014. Due to lack of data, we are unable to show the decline phase of this cycle.

At the maximum phase of this cycle in 2014, the sunspot number was around 100 and this value declines from 2015. The value of  $R$  in the solar cycle 24 has a low peak, which means we might expect a low surface absorption of solar energy compared to that at peaks of solar cycle 22 and 23. We found different sunspot cycle periods, representing the time elapsed from one minimum that precedes its maximum to another minimum that follows its maximum. This definition doesn't consider the fact that each cycle starts well before the preceding minimum and continues well after the following minimum. By the above definition, the sunspot cycle has its period depending on the behavior of the preceding as well as the following cycles [Hathaway, 2015].

According to Eddy [1977], cycle periods don't appear to be normally distributed. According to Wilson [1987], a bimodal distribution is required to fit the data with the short-period cycle of 122 months and the long-period cycles of 140 months separated by the Wilson Gap that surrounds the mean cycle-length of 132.7 months. In contrast, Hathaway et al. [2002] reported that the distributions of cycle periods were normal with a mean of 131 months. Feminella and Storini [1997] further supported this concept and noted that such phenomena are particularly clear in large events. Norton and Gallagher [2010] later concluded that the Gnevyshev gap occurs in both hemispheres and is not the result of superposition of two out-of-phase hemispheres. Waldmeier [1935, 1939] suggested that the time taken by sunspot number to reach maximum from minimum is inversely proportional to the amplitude of the cycle and this relationship is called Waldmeier Effect. Even though this effect is widely accepted, it has certain problems. Hathaway et al. [2002] suggested that such effect was greatly reduced by the use of group sunspot numbers.

The second panel of Figure 1 represents the variation of solar wind temperature during the period of solar cycle. During the rise and maximum phase of each solar cycle, the solar wind temperature increases. But we have found its significant peak during the decline phase of solar cycle 22 and 23. The presence of significant peaks of temperature during the decline phase of solar cycle signifies the resultant effect of increasing sunspot numbers and area during the rise and maximum phase of the same so-

lar cycle. It suggests that the geomagnetic storm caused by the ejection of huge magnetic structures from larger sunspots during the maximum and decline phase has high plasma temperature.

[*Hayakawa et al., 2017*] mention that the wider sunspots eject several huge sequential magnetic structures into interplanetary space, resulting into unusual storm activity. Higher the solar activity higher will be the solar wind temperature. Solar variability can cause an adverse effect on Earth's environment and global climate. Solar activity's grand maximum in 20th century seems to have come to an end, leading to comparatively lower solar activity predictions for few upcoming decades [*Clilverd et al., 2006; de Jager and Duhau, 2009; Lockwood et al., 2009*]. According to *Feulner and Rahmstorf [2010]*, a new grand minimum in solar activity will result in fall of mean global temperature by just  $0.1^{\circ}\text{C}$  (or probably  $0.3^{\circ}\text{C}$  if uncertainties in the model are considered). Comparing to the  $3.7$  to  $4.5^{\circ}\text{C}$  temperature rise expected from greenhouse emissions, such a decrease is a minor one [*Feulner and Rahmstorf [2010]*]. Similarly, *Jones et al. [2012]* predicted a global temperature decrease of  $0.06$  to  $0.1^{\circ}\text{C}$  because of solar activity. Recently, *Solheim et al. [2012]* suggested the correlation between the length of the solar cycle and the North Atlantic temperatures during the following solar cycle. According to *Xoplaki et al. [2005]*, total solar irradiance (TSI) variations could be major reasons behind the coldest springs observed during Maunder Minimum (long periods having low solar activity). A hypothesis regarding the aid of cosmic rays on cloud formation is a possible link between the climate change and solar activity as those clouds enhance the greenhouse effect and change Earth's albedo [*Lockwood, 2012*]. Such a phenomenon can influence the Earth's temperature. *Svensmark and Friis-Christensen [1997]*, who claimed that a net negative radiative forcing is exerted by the cloud cover, confirmed a strong correlation between cloud cover and solar activity. However, some authors suggested that cloud optical thickness wasn't taken into account in such study [*Jorgensen and Hansen, 2000*].

Correlations between Earth's surface temperature and TSI variation in the 11-year cycle have been studied in the last few decades to deduce a casual relation. However, such correlations are problematic because many climate forcing factors

like: greenhouse gases, aerosol concentrations, etc. have considerably varied over the last few decades [*Engels and Geel, 2012*]. According to *Xoplaki et al. [2005]*, TSI variations could be major reason behind the coldest springs observed during Maunder Minimum (long periods having low solar activity). [*Foukal et al., 2006; Fröhlich, 2006; Yeo et al., 2014*] mention that TSI alone cannot explain observed climate variations. During that period the average winter temperatures in some western European countries (main data from England, France, and the Netherlands) were below average. This observation has led to the suggestion that solar activity and climate can be correlated. Even though many phenomena control climate on the longer timescales, small-scale short energy balance variations in the Sun can lead to non-linear large responses like variations in atmospheric circulation or thermohaline circulation perturbations [*Martin-Puertas et al., 2012*]. Hence, improved knowledge of the natural variability including solar variability will be needed to understand the anthropogenic effects upon the Earth's climate.

The third panel of Figure 1 represents the variation of solar wind velocity. We found significant peaks of solar wind velocity during the decline phase of each solar cycle which suggests the occurrence of geomagnetic storm in that period. This also shows that there is high chance of occurrence of geomagnetic storm during the maximum and decline phase of the solar cycle. Statistically, there is 0.5 CME per day during solar minimum whereas 6 per day during maximum [*Gopalswamy et al., 2003*]. The fourth panel of Figure 1 represents the magnetic field ( $B$ ) perturbation during the solar cycle period. We found that during each solar cycle, the value of  $B$  increases along the rising phase, remains almost constant along the maximum phase, and decreases along decline phase. It suggests that there is some correlation between the magnetic field variation and different phases of the solar cycle. The fifth panel of Figure 1 represents the perturbation of IMF north-south component. We found that the north-south component perturbation is independent of the phases of solar cycle. But we can conclude that the perturbation of  $B_z$  can occur during the geomagnetic storm.

According to *Lemaire and Singer [2012]*, southward IMF  $B_z$  allows entry of charged particles i.e. including cosmic rays. This means a positive corre-

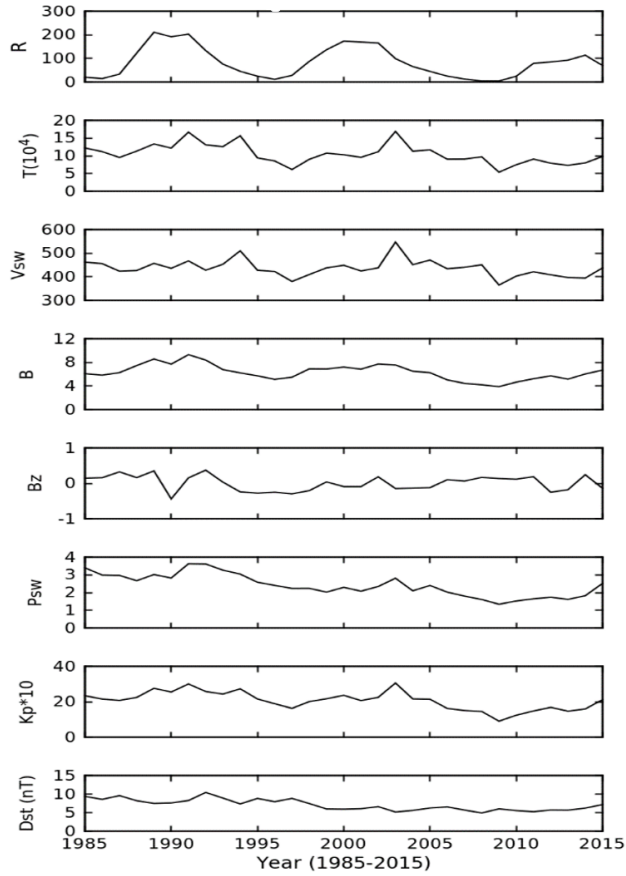


**Figure 1.** Yearly values of sunspots number ( $R$ ), Solar wind velocity ( $V_{sw}$ ), Magnitude of magnetic field ( $B$ ), North-south component of interplanetary magnetic field ( $B_z$ ), Solar wind Plasma Pressure ( $P_{sw}$ ),  $Kp$  and  $Dst$  indices from 1985–2015.

lation exists between IMF  $B_z$  and cosmic ray flux. Here, we have observed some anti-correlation of IMF  $B_z$  with sunspot number. Our work also supports the claim by *Utomo* [2017] that the cosmic rays have a near anti-correlation with sunspot numbers. The sixth panel of Figure 1 represents the solar wind plasma pressure perturbation. We found that solar wind plasma pressure increases during decline phase of solar cycle in the same way as solar wind velocity. The seventh panel of Figure 1 represents the perturbation of  $Kp$  index. The fluctuation pattern of  $Kp$  index shows its periodic nature with respect to the three phases of each solar cycle. Hence  $Kp$  index is one of the good indicators of solar active period. The bottom panel represents the  $Dst$  index fluctuation during the solar cycle and its fluctuation suggests no distinct pattern.

Similarly, Figure 2 represents the yearly values of

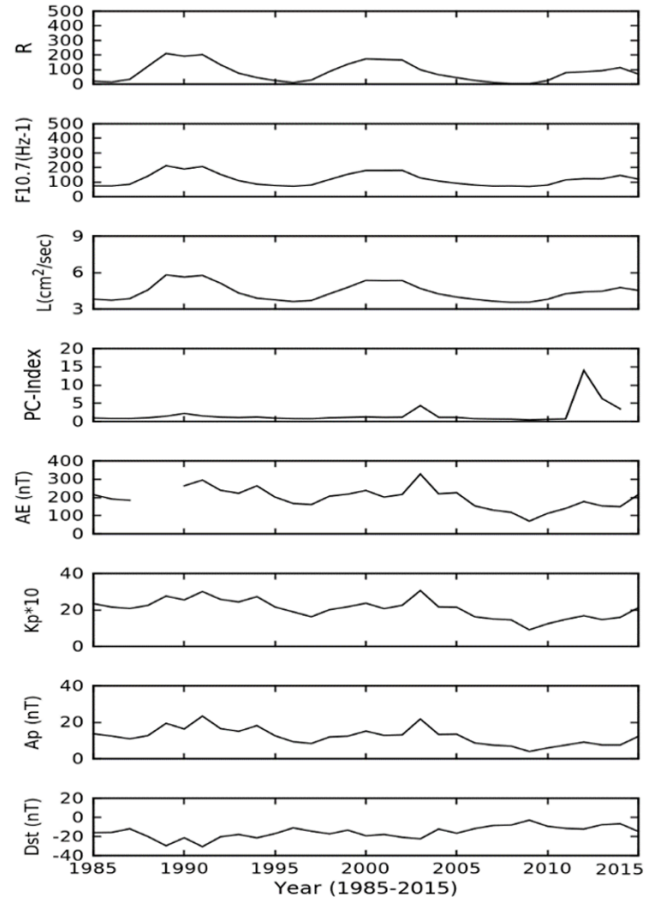


**Figure 2.** Yearly values of sunspots number ( $R$ ), solar flux ( $F_{10.7}$ ), Lyman Alpha ( $L$ ),  $PC$ ,  $AE$ ,  $Kp$ ,  $Ap$  and  $Dst$  indices for the same periods from 1985–2015.

sunspots number ( $R$ ), solar flux ( $F_{10.7}$ ), Lyman Alpha ( $L$ ),  $PC$ ,  $AE$ ,  $Kp$ ,  $Ap$  and  $Dst$  indices for the same periods. The first panel of Figure 1 and Figure 2 are same. The second and third panel of Figure 2 represents the fluctuation of solar flux ( $F_{10.7}$ ) and Lyman Alpha ( $L$ ) indices during the phases of solar cycle respectively. We found that the sunspot number, solar flux index ( $F_{10.7}$ ) and Lyman Alpha ( $L$ ) shows periodic trend during every 11 years. However, the last solar cycle (2008–2015) shows minimum as compared to previous two. We observed the solar cycle dependence on solar flux index and found a strong dependence on solar activity. Hence, solar flux index,  $F_{10.7}$  and Lyman Alpha are an excellent indicator of solar magnetic activity. The fourth panel of Figure 2 represents the polar cap index (PCI) fluctuation and it has the maximum fluctuation in the latest solar cycle

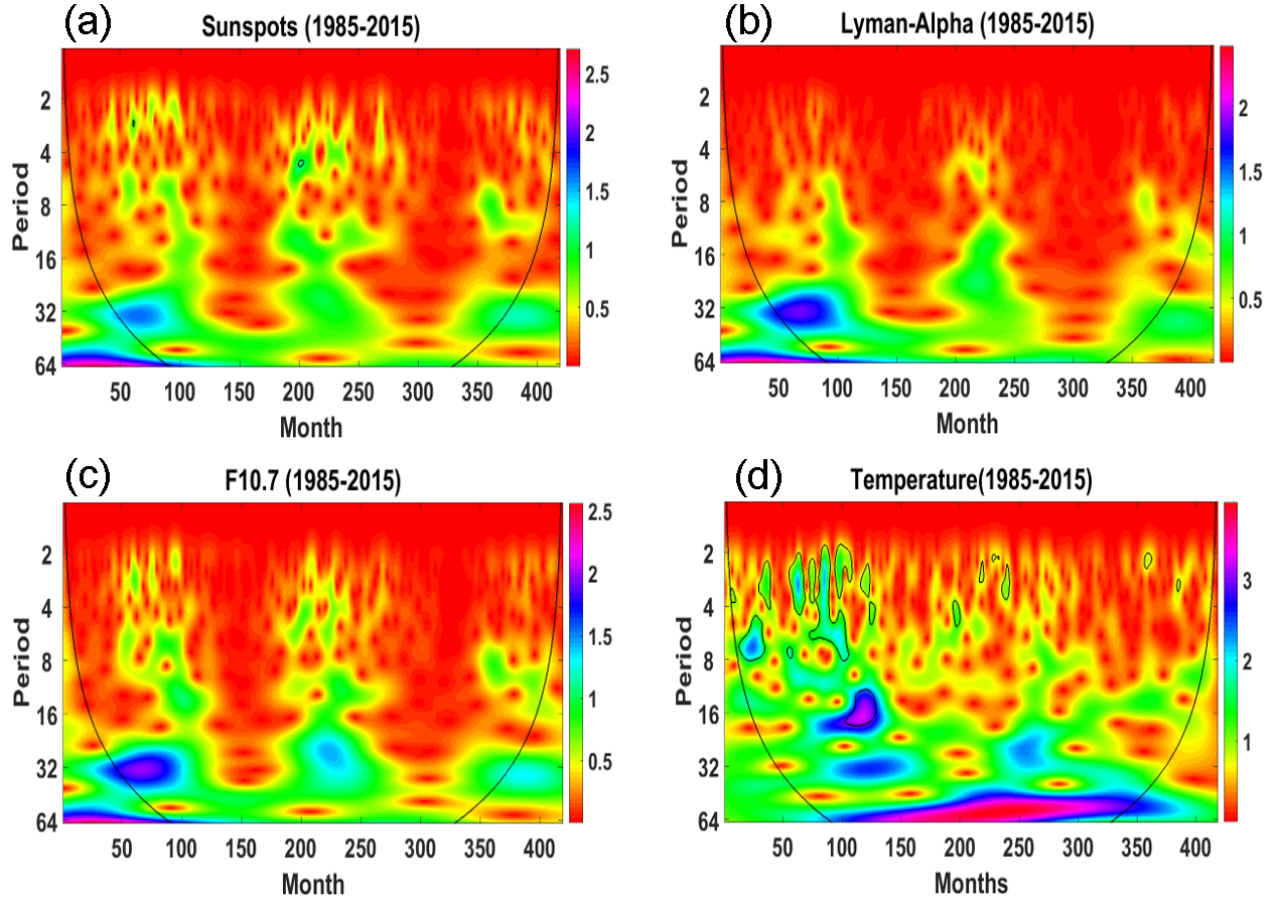


**Figure 3.** Scalograms for Lyman Alpha ( $L$ ), Solar flux ( $F_{10.7}$ ), sunspots number ( $R$ ) and solar wind temperature ( $T$ ) from 1985–2015.

i.e. solar cycle 24. It is because PCI and polar cap voltage (PCV) are correlated [Adhikari *et al.*, 2018], this means that there is a big difference between the maximum and minimum electronic convection potential in ionosphere during this period.

In the solar cycle 24, the Sun’s polar fields had low magnitude compared to cycle 22 and 23 [Basu, 2013]. This means that low solar polar fields correspond to the highest difference between the highest and the lowest value of electronic convection potential. The fifth panel of Figure 2 represents the  $AE$  index perturbation and we have found that the fluctuation pattern of  $AE$  index is similar to the solar wind velocity and solar wind plasma pressure variation. The fluctuation pattern of  $Ap$  index in the seventh panel of Figure 2 is similar to the  $Kp$  index and the bottom panel of Figure 2 represents the perturbation of  $Dst$  index. We found that  $Dst$  can vary during the phases of solar cycle and it also represents the solar active period.

## Continuous Wavelet Transform

In wavelet analysis, scalogram can analyze a signal in a time-scale plane. In all the diagrams of Figure 3, the horizontal axis represents the time in months and the vertical axis represents the periodicity in minutes. Analogous to Fourier analysis, the square modulus of the wavelet coefficient provides energy distribution in the time-scale plane. We can explore the central frequencies or central periods of the time series called pseudo-frequencies or pseudo-periods. This helps to understand the behavior of the energy spectrum at a certain scale [Klausner *et al.*, 2013]. On the scalogram, stronger wavelet power areas are shown in pink and weaker wavelet power areas are shown in red. Breaking down the scalograms, the characteristic of signal demonstrates high variability in time without the presence of continuous periodicities. Figure 3 shows

the Scalograms for Lyman Alpha ( $L$ ), solar flux index ( $F_{10.7}$ ), sunspots number ( $R$ ) and solar wind temperature ( $T$ ) and we also observed periodicities on solar flux index using wavelet analysis. Through this analysis, it was found that the power intensities of sunspot number, solar flux index and Lyman Alpha shows a high spectral variability. This study mainly focused on the variation of sunspot number, solar flux index, Lyman Alpha and plasma temperature from 1985–2015. We observed the solar cycle dependence on solar flux index and found a strong dependence on solar activity. Results also show that solar intensities are higher during the rising phase and maximum phase of the solar cycle. We found that solar flux, sunspot number and Lyman Alpha all have highest spectral variability from 0 to 100 months. We observed a power area of period 4 to 8 for temperature on the 30th month. This period corresponds to the rising phase of solar cycle 22, a power area of period 16 for temperature on the 100th month which was observed during the decline phase of solar cycle 22. Temperature, however, has highest spectral variability from 100 to 380 months and this period corresponds to solar cycle 23.

Sunspot number, Lyman Alpha and  $F_{10.7}$  all have continuous spectral energy of medium to low magnitude. Temperature, however, has a continuous spectral energy of all magnitudes at different frequencies. In both the cases, the low spectral energy of medium and high frequency are discontinuous. The continuous periodicity observed for solar wind temperature from 100 to 380 months suggests that during this period the solar activity was high. Hence, we found that due to the continuous solar wind temperature increment during different phases of solar cycle over a long period can cause global climate change. Primarily, solar variability affects the global climate by directly influencing the global energy balance. On average, the global temperature rise is about  $0.07^{\circ}\text{C}$  during 11-year maximum and minimum period [Gray et al., 2010]. However, surface temperature changes are spatially diverse and changes in regional temperature are much greater compared to  $0.07^{\circ}\text{C}$  [Gray et al., 2010]. The bottom-up mechanism and uptake of solar heat by oceans amplifies the effects of solar activity on climate [Gray et al., 2010; Meehl et al., 2008, 2009]. When atmospheric circulation is strengthened, subtropical subsidence gets

enhanced, which further decreases during the formation of cloud and increases as the surface absorbs solar energy [Gray et al., 2010; Meehl et al., 2008, 2009]. Rahoma and Helal [2013] found that solar activity has a direct impact on the rise of air temperature and affects relative humidity.

## Cross-Correlation

A statistical measure of the relation between two variables as a function of a time-lag applied to one of them and is known as cross-correlation [Mannucci et al., 2008]. This allows us to check the interaction between two sets of data for each considered scale. It is generally used to measure information between two different time series [Usoro, 2015; Adhikari et al., 2017]. The closer positive cross-correlation value is 1 [Katz, 1988], so we use Pearson's correlation coefficient that ranges from  $-1$  to  $+1$ . The portion of the curves near  $-1$  and  $+1$  depict good linear fit and highest correlation whereas those near 0 depict poor fit and less correlation [Katz, 1988]. The horizontal axis in the graph shows the time ranging from  $-30$  to  $+30$  years.

Figure 4 represents the cross-correlation between sunspot numbers ( $R$ ) and other parameters: North-south component of interplanetary magnetic field ( $B_z$ ), Magnitude of magnetic field ( $B$ ), solar flux ( $F_{10.7}$ ), Lyman Alpha ( $L$ ), solar wind plasma pressure ( $P_{sw}$ ), solar wind velocity ( $V_{sw}$ ), and solar wind plasma temperature ( $T$ ). The  $R - F_{10.7}$  (red line) has high and positive amplitude, which means a positive correlation. The red line reached the highest positive cross-correlation coefficient of 1 at lag zero. The  $R - L$  (sky blue line) also shows a positive correlation with cross-correlation coefficient of 0.82 at lag zero. The red and sky blue lines are in same phase showing the solar cycle dependence on solar flux index and Lyman Alpha. Hence solar flux index ( $F_{10.7}$ ) and Lyman Alpha ( $L$ ) are an excellent indicator of solar magnetic activity. The  $R - P_{sw}$  (pink line),  $R - V_{sw}$  (yellow line), and  $R - T$  (black line) show positive correlation with coefficient around 0.8 at nearly zero time lag. These lines are sometimes overlapped with each other which indicates that increasing solar activity creates a high chance of occurrence of

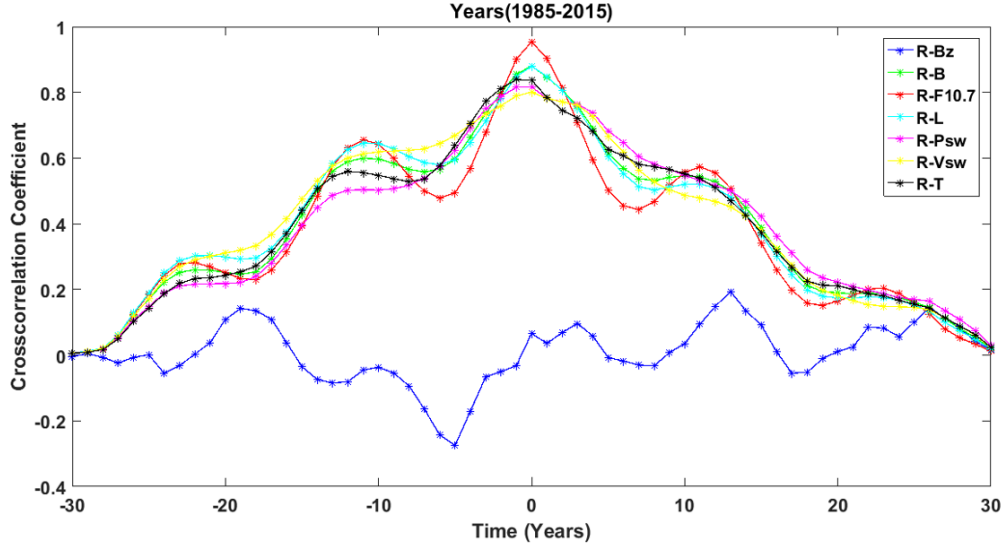


**Figure 4.** Cross-correlation between  $R$  with  $B_z$  (blue),  $B$  (green),  $F_{10.7}$  (red),  $L$  (sky blue),  $P_{sw}$  (pink),  $V_{sw}$  (yellow) and  $T$  (black) from 1985–2015.

geomagnetic storm. Hence, the solar wind parameters variation depends on the intensity of magnetic structure ejected from the sunspot.

*Rathore et al.* [2012] found that the annual occurrence of geomagnetic storm is strongly correlated with 11-year sunspot cycle. They also found that Halo CME is the main cause of the production of a geomagnetic storm. The  $R - B$  (green line) shows same nature as pink, yellow and black. This means that magnetic structure ejected from sunspot interacts with Earth magnetic field and results in perturbation of total magnetic field of the Earth. The  $R - B_z$  (blue line) also shows moderate correlation with cross-correlation coefficient highly fluctuating around 0 which is an interesting result to be noticed. It can be possible because  $B_z$  is just a component and total magnetic field ( $B$ ) shows a positive correlation with  $R$ . Here less correlated line seems to be more irregular and fluctuating than the highly correlated ones. The above findings suggest that the structure and intensity of the solar wind plasma depend upon the number and size of sunspots whereas, the solar wind parameter variation depends on the size of magnetic structure being ejected during solar activity. The most remarkable result to emerge from our study is the fact that huge magnetic structure ejected during solar activity carry solar energy and deposit it to global environment which leads to interplanetary parameter variation.

Figure 5 represents the cross-correlation between sunspot numbers ( $R$ ) and other parameters: PCI,  $AE$ ,  $Kp$ ,  $Ap$ , and  $Dst$ . The  $R - Kp$  (sky blue line),  $R - Ap$  (pink line) and  $R - AE$  (red line) show high positive correlation with cross-correlation coefficient around 0.88 at zero lag. These three lines sometimes overlap with each other. The  $R - Dst$  (yellow) shows a positive correlation with a coefficient of around 0.8 at time +5 years. The  $R - PCI$  (blue line) reveals highly fluctuating nature with the maximum and minimum coefficient of around 0.65 and 0.17. Hence the sunspot number shows good correlation with all indices except the polar cap.

## Conclusion

Virtually, the Sun ejects magnetized plasma repeatedly into space. The solar wind and the Coronal Mass Ejections are two components which contribute to the formation of sunspots and are able to populate a large fraction of the inner heliosphere with accelerated ions. The occurrence of these events indicate a solar active period. The effect of solar activity on global climate variation remains an important issue, yet somewhat controversial. Our work somehow tries to minimize this controversy.

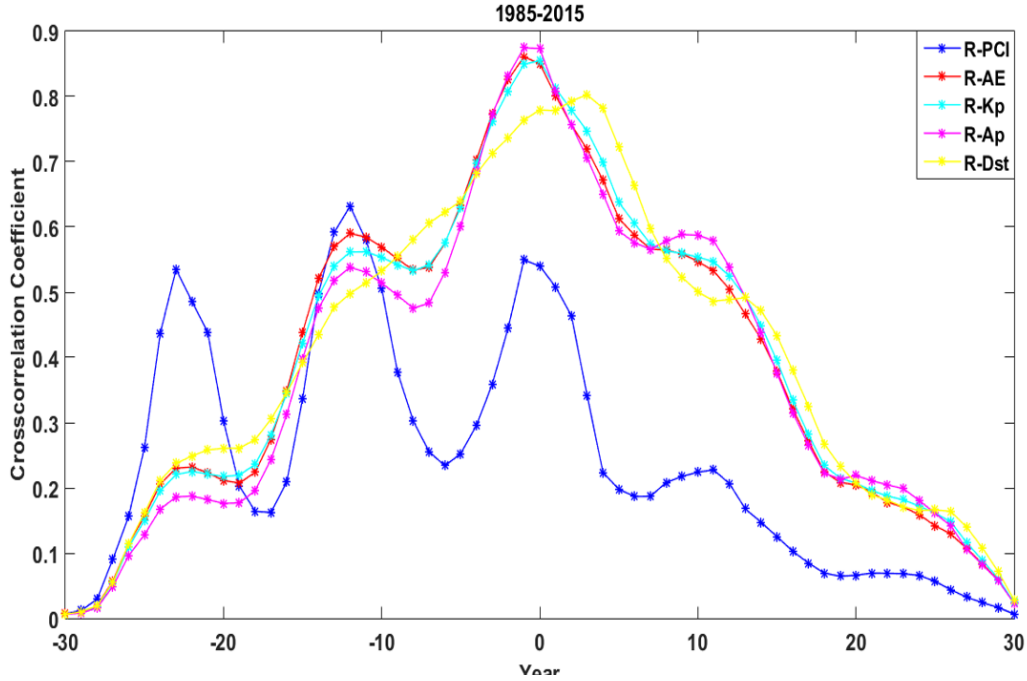


**Figure 5.** Cross-correlation of  $R$  with PCI (blue),  $AE$  (red),  $Kp$  (sky blue),  $Ap$  (pink), and  $Dst$  (yellow) from 1985–2015.

We have found a positive correlation between plasma temperature ( $T$ ) and sunspot numbers ( $R$ ). Our result clearly shows the effect of rising phase (higher  $R$  number) of the solar cycle on plasma temperature variation. The plasma temperature variation directly depends upon the magnetic structure ejected from sunspots. We found the increasing trend of  $R$  during the rising phase of solar cycle increases the global temperature due to energy deposition carried by solar wind plasma. The overall effect can be seen in the following years as well in the form of an intense geomagnetic storm. We can conclude that the continuous rise of solar wind temperature for a long period can have an adverse effect on global climate. This result is in accordance with [Lockwood \[2009\]](#) and [Weber \[2010\]](#), who stated that there is a small, but noticeable influence of solar activity on the climate on longer time scales particularly on global temperature variation.

Many researchers claim that the solar activity has some role in global temperature variation but the increasing anthropogenic activity masks its effect. [Engels and Geel \[2012\]](#): many climate forcing factors like greenhouse gases, aerosol concentrations, etc. have considerably varied over the last few decades. The daily geomagnetic activities that

occur during solar cycle indicate the continuous deposition of solar energy carried by plasma from heliosphere. When solar absorption increases by bottom-up mechanism, evaporation also increases and it results in an increase of moisture converging to the precipitation regions and so, the precipitation maxima becomes high. Because of intensified maxima of precipitation and related upward vertical motions, stronger trade winds along with greater Pacific Ocean upwelling are seen in equatorial region [[Gray et al., 2010](#)]. The value of  $R$  in the solar cycle 24 has a low peak, which means we might expect a low surface absorption of solar energy compared to that at peaks of solar cycle 22 and 23. Hence, we conclude that the solar activity causes global mean temperature change but its value is low.

Through CWT, we found that solar flux, sunspot number, and Lyman Alpha all have highest spectral variability from 0 to 100 months. Temperature, however, has highest spectral variability from 100 to 380 months. Sunspot number, Lyman Alpha, and  $F_{10.7}$  show a continuous spectral energy of medium and low magnitude. Temperature, however, has a continuous spectral energy of all magnitudes at different frequencies. In both cases, the

low spectral energy of medium and low frequencies are discontinuous. Sunspot numbers ( $R$ ),  $F_{10.7}$  and  $L$  show similar periodicity in solar cycle 24 as well, but the peak is low. However, PCI has maximum value in the latest solar cycle. We found a positive correlation between PCI and PCV. This result is also mentioned in *Adhikari et al. [2018]* which indicates that there is a big difference between the maximum and minimum electronic convection potential in ionosphere during this period. In the solar cycle 24, the Sun polar field had low magnitude compared to cycle 22 and 23 as mentioned in [*Basu, 2013*]. This low solar polar field corresponds to the highest difference between electronic convection potentials. The same low solar polar field also corresponds to low values in  $R$ ,  $F_{10.7}$ , and  $L$ .

**Acknowledgments.** The solar, interplanetary, and geomagnetic (SIG) parameters for this study were obtained from <https://omniweb.gsfc.nasa.gov/>. The author thanks for them. B. Adhikari acknowledges Research Grant FY 2017/2018 from Nepal Academy of Science and Technology (NAST).

## References

- Adhikari, B., S. Dahal, N. P. Chapagain (2017), Study of field-aligned current (FAC), *Earth and Space Science*, 4, No. 5, 257–274, [Crossref](#)
- Adhikari, B., N. Sapkota, B. Bhattarai, et al. (2018), Study of interplanetary parameters, polar cap potential, and polar cap index during quiet event and high intensity long duration continuous AE activities (HILDCAAs), *Russian Journal of Earth Sciences*, 18, No. 1, ES1001, [Crossref](#)
- Basu, S. (2013), The peculiar solar cycle 24 – where do we stand?, *Journal of Physics: Conference Series*, IOP Publishing, 440, No. 1, 012001, [Crossref](#)
- Berger, A. (1988), Milankovitch theory and climate, *Reviews of Geophysics*, 26, No. 4, 624–657, [Crossref](#)
- Caprioli, D., E. Amato, P. Blasi (2010), The contribution of supernova remnants to the galactic cosmic ray spectrum, *Astroparticle Phys.*, 33, 160–168, [Crossref](#)
- Chattopadhyay, G., S. Chattopadhyay (2012), Monthly sunspot number time series analysis and its modeling through autoregressive artificial neural network, *Eur. Phys. J. Plus*, 127, 1–8, [Crossref](#)
- Clilverd, M. A., E. Clarke, T. Ulich, H. Rishbeth, M. J. Jarvis (2006), Predicting solar cycle 24 and beyond, *Space Weather*, 4, No. 9, 1–7, [Crossref](#)
- Daubechies, I. (1992), Ten Lectures on Wavelets, *CBMS-NSF Regional Conference (Series in Applied Mathematics)*, Vol. 61 p.17–107, SIAM, Philadelphia, PA.
- De Jager, C. (2005), Solar forcing of climate. 1: Solar variability, *Space Science Reviews*, 120, No. 3–4, 197–241, [Crossref](#)
- De Jager, C., S. Duhau (2009), Forecasting the parameters of sunspot cycle 24 and beyond, *Journal of Atmospheric and Solar-Terrestrial Physics*, 71, No. 2, 239–245, [Crossref](#)
- Domingues, M. O., O. J. Mendes, A. C. Mendes (2005), On wavelet techniques in atmospheric sciences, *Advances in Space Research*, 35, 831–842, [Crossref](#)
- Engels, S., B. van Geel (2012), The effects of changing solar activity on climate: contributions from palaeoclimatological studies, *Journal of Space Weather and Space Climate*, 2, A09, [Crossref](#)
- Eddy, J. A. (1976), The Maunder Minimum, *Science*, 192, 1189–1202, [Crossref](#)
- Eddy, J. A. (2009), *The Sun, the Earth, and Near-Earth Space: A Guide to the Sun-Earth System*, 20402-0001 pp. Government Printing Office, Washington, DC.
- Eddy, J. A. (1976), Climate and the changing sun, *Climatic Change*, 1, No. 2, 173–190, [Crossref](#)
- Feminella, F., M. Storini (1997), Large-scale dynamical phenomena during solar activity cycles, *Astronomy and Astrophysics*, 322, 311–319.
- Feulner, G., S. Rahmstorf (2010), On the effect of a new grand minimum of solar activity on the future climate on Earth, *Geophysical Research Letters*, 37, No. 5, 1–4, [Crossref](#)
- Foukal, P., C. Fröhlich, H. Spruit, T. M. L. Wigley (2006), Variations in solar luminosity and their effect on the Earth’s climate, *Nature*, 443, No. 7108, 161, [Crossref](#)
- Fröhlich, C. (2006), Solar irradiance variability since 1978, *Solar Variability and Planetary Climates* p.53–65, Springer, New York, NY.
- Gopalswamy, N., M. Shimojo, W. Lu, et al. (2003), Prominence eruptions and coronal mass ejection: a statistical study using microwave observations, *Astrophysical Journal*, 586, No. 1, 562, [Crossref](#)
- Gray, L. J., J. Beer, M. Geller, et al. (2010), Solar influences on climate, *Reviews of Geophysics*, 48, No. 4, 24–26, [Crossref](#)
- Grossmann, A., J. Morlet (1983), Decomposition of Hardy functions into square integrable wavelets of constant shape, *SIAM Journal on Mathematical Analysis*, 15, 723–73, [Crossref](#)
- Hathaway, D. H. (2015), The solar cycle, *Living Reviews in Solar Physics*, 12, No. 4, 12–28, [Crossref](#)
- Hathaway, D. H., R. M. Wilson, E. J. Reichmann (2002), Group sunspot numbers: sunspot cycle characteristics, *Solar Physics*, 211, No. 1–2, 357–370, [Crossref](#)
- Hayakawa, H., K. Iwahashi, Y. Ebihara, H. Tamazawa,

- et al. (2017), Long-lasting Extreme Magnetic Storm Activities in 1770 Found in Historical Documents, *Astrophys. J. Lett.*, 850, No. 2, 2–5.
- Herschel, W. (1801), Observations tending to investigate the nature of the Sun ..., *Philosophical Transactions of the Royal Society of London*, 91, 265–318, **Crossref**
- Jones, G. S., M. Lockwood, P. A. Stott (2012), What influence will future solar activity changes over the 21st century have on projected global near-surface temperature changes?, *Journal of Geophysical Research: Atmospheres*, 117, No. D5, 4–11, **Crossref**
- Jorgensen, T. S., A. W. Hansen (2000), Comments on "Variation of cosmic ray flux and global cloud coverage—a missing link in solar-climate relationships", *Journal of Atmospheric and Solar-Terrestrial Physics*, 62, No. 1, 73–77, **Crossref**
- Katz, R. W. (1988), Use of cross correlations in the search for teleconnections, *J. Climatology*, 8, 241–253, **Crossref**
- Kilcik, A., V. B. Yurchyshyn, A. Ozguc, J. P. Rozelot (2014), Solar cycle 24: Curious changes in the relative numbers of sunspot group types, *Astrophysical Journal Letters*, 794, No. 1, L2, **Crossref**
- Klausner, V., A. R. Papa, O. Mendes, et al. (2013), Characteristics of solar diurnal variations: A case study based on records from the ground magnetic station at Vassouras, Brazil, *Journal of Atmospheric and Solar-Terrestrial Physics*, 92, 124–136, **Crossref**
- Lemaire, J. F., S. F. Singer (2012), What happens when the geomagnetic field reverses?, *Dynamics of the Earth's Radiation Belts and Inner Magnetosphere, Geophysical Monograph Series* p.355–364, AGU, Washington, USA. **Crossref**
- Lockwood, M., A. P. Rouillard, I. D. Finch (2009), The rise and fall of open solar flux during the current grand solar maximum, *Astrophysical Journal*, 700, No. 2, 937, **Crossref**
- Lockwood, M. (2009), Solar change and climate: an update in the light of the current exceptional solar minimum, *Proceedings of the Royal Society of London A: Mathematical, Physical and Engineering Sciences* p.rspa20090519, The Royal Society, London.
- Lockwood, M. (2012), Solar influence on global and regional climates, *Surveys in Geophysics*, 33, No. 3–4, 503–534, **Crossref**
- Mannucci, A. J., B. T. Tsurutani, M. A. Abdu, et al. (2008), Superposed epoch analysis of the dayside ionospheric response to four intense geomagnetic storms, *Journal of Geophysical Research: Space Physics*, 113, No. A3, 8–10, **Crossref**
- Meehl, G. A., J. M. Arblaster, G. Branstator, H. Van Loon (2008), A coupled air–sea response mechanism to solar forcing in the Pacific region, *Journal of Climate*, 21, No. 12, 2883–2897, **Crossref**
- Meehl, G. A., J. M. Arblaster, K. Matthes, F. Sassi, H. van Loon (2009), Amplifying the Pacific climate system response to a small 11-year solar cycle forcing, *Science*, 325, No. 5944, 1114–1118, **Crossref**
- Martin-Puertas, C., K. Matthes, A. Brauer, et al. (2012), Regional atmospheric circulation shifts induced by a grand solar minimum, *Nature Geoscience*, 5, No. 6, 397, **Crossref**
- Milankovitch, M. (1941), *History of Radiation on the Earth and its Use for the Problem of the Ice Ages*, K. Serb. Akad., Beogr.
- Morlet, J. (1983), Sampling theory and wave propagation, *Acoustic Signal/Image Processing and Recognition*, (ed C. Chen) p.233–261, Springer-Verlag, New York.
- Norton, A. A., J. C. Gallagher (2010), Solar-Cycle Characteristics Examined in Separate Hemispheres: Phase, Gnevyshev Gap, and Length of Minimum, *Solar Physics*, 261, No. 1, 193, **Crossref**
- Rahoma, U. A., R. Helal (2013), Influence of Solar Cycle Variations on Solar Spectral Radiation, *Atmospheric and Climate Sciences*, 3, No. 01, 47–54, **Crossref**
- Rathore, B. S., S. C. Kaushik, R. S. Bhadoria, K. K. Parashar, D. C. Gupta (2012), Sunspots and geomagnetic storms during solar cycle-23, *Indian Journal of Physics*, 86, No. 7, 563–567, **Crossref**
- Solheim, J. E., K. Stordahl, O. Humlum (2012), The long sunspot cycle 23 predicts a significant temperature decrease in cycle 24, *Journal of Atmospheric and Solar-Terrestrial Physics*, 80, 267–284, **Crossref**
- Solomon, S., et al. (eds.) (2007), *Climate Change 2007, The Physical Science Basis-Contribution of Working Group I to the Fourth Assessment Report of the Intergovernmental Panel on Climate Change* p.663–745, Cambridge Univ. Press, Cambridge, UK.
- Svensmark, H., E. Friis-Christensen (1997), Variation of cosmic ray flux and global cloud coverage – a missing link in solar-climate relationships, *Journal of Atmospheric and Solar-Terrestrial Physics*, 59, No. 11, 1225–1232, **Crossref**
- Usoro, A. E. (2015), Some basic properties of cross-correlation functions of n-dimensional vector time series, *J. Stat. Econ. Methods*, 4, No. 1, 63–71.
- Usoskin, I. G., K. Mursula (2003), Long-term solar cycle evolution: review of recent developments, *Solar Physics*, 218, No. 1–2, 319–343, **Crossref**
- Utomo, Y. S. (2017), Correlation analysis of solar constant, solar activity and cosmic ray, *Journal of Physics: Conference Series, IOP Publishing*, 817, No. 1, 012045, **Crossref**
- Vandenberghe, J., R. Coope, K. Kasse (1998), Quantitative reconstructions of palaeoclimates during the last interglacial-glacial in western and central Europe: an introduction, *Journal of Quaternary Science*, 13, No. 5, 361–366, **Crossref**
- Waldmeier, M. (1935), New features of the sunspot curve, *Astronomical Communications of the Swiss Federal Observatory Zurich*, 14, 105–136.
- Waldmeier, M. (1939), The zonal migration of the sunspots, *Astronomical Communications of the Swiss Federal Observatory Zurich*, 14, 470–481.
- Weber, W. (2010), Strong signature of the active Sun in 100 years of terrestrial insolation data, *Annalen der*

*Physik*, 522, No. 6, 372–381, **Crossref**  
Wilson, R. M. (1987), On the distribution of sunspot cycle periods, *Journal of Geophysical Research: Space Physics*, 92, No. A9, 10,101–10,104, **Crossref**  
Xoplaki, E., J. Luterbacher, H. Paeth, D. Dietrich, N. Steiner, M. Grosjean, H. Wanner (2005), European spring and autumn temperature variability and change of extremes over the last half millennium, *Geophysical Research Letters*, 32, No. 15, 2–3, **Crossref**

Yeo, K. L., N. A. Krivova, S. K. Solanki (2014), Solar cycle variation in solar irradiance, *Space Science Reviews*, 186, No. 1–4, 137–167, **Crossref**

---

**Corresponding author:** Binod Adhikari, Department of Physics, St. Xavier's College, Maitighar, Kathmandu, Nepal (binod.adhi@gmail.com)